Desalination, 86 (1992)
Elsevier Science Publishers B.V., Amsterdam

Studies on polarity reversal with continuous deionization

YORAM OREN* and YAIR EGOZY

Millipore Co., Bedford, Massachusetts 01730 (USA)

(Received November 5, 1991; in revised form February 5, 1992)

SUMMARY

A continuous deionization (CDI) module was constructed with all intermembrane spaces filled with mixed bed ion exchange resins, and was operated under polarity reversal conditions. The system was operated on feeds with and without scale-forming components as a function of the frequency of polarity reversal and applied voltage. Conductivity and pH profiles along the module and water quality obtained from the system were monitored and analyzed, based on water splitting and ion transfer throughout the system. Sensitivity to scale and recommended operating conditions are discussed.

INTRODUCTION

Continuous deionization (CDI)

Continuous deionization, also known as electrodeionization process, uses ion exchange membranes and resins to deionize fluids. In this process, ions are driven out of the solution under the influence of an electric field, and

---

*On leave (1988-89) from the Chemistry Department, Nuclear Research Center-Negev, POB 9001, Beer Sheva 84190, Israel.

there is no need for chemical regeneration of the ion exchange resins. Electrodeionization has been reported in the literature since 1955 when Walters et al. [1] proposed it for concentration of radioactive wastes. Early devices were also proposed, among others [2–6].

The first commercially available system was introduced by the Millipore Corporation in 1987. It was described by Ganzi et al. [7] as a process for the production of high purity water (above 1 Megohm-cm) from potable sources. With further improvements in module design and a better understanding of the process, it has been possible to produce water with a resistivity of 15–17 megohm-cm in a consistent manner [8–10].

The scale problem

Like other membrane deionization processes, CDI modules have to be protected from scale formation. In any such process (e.g., reverse osmosis), the feed water is separated into at least two streams: the product water with ionic concentration lower than that of the feed, and a waste stream in which the ionic contaminants *concentrate*. If the feed water contains ions such as calcium and carbonate and the concentration in the feed is close to the saturation point, there is a risk that the concentration of those ions will exceed the solubility product threshold, and scale will be formed.

The sensitivity to scale is usually estimated by the Langelier Saturation Index (LSI), which at 25°C is [11]:

$$LSI = 0.995 \log [Ca^{++}] + 0.016 \log[Mg^{--}] + 1.041 \log [HCO_3^-] - 0.197 \log[S] + pH - 11.017$$

where S is the total dissolved solids (TDS) and all the concentrations are in ppm units.

If local conditions are such that the LSI is positive, the unit is likely to form scale; and if the LSI is negative, the probability of scale formation is low. It should be noted, however, that local conditions may be such that scale could be formed within a module even when the overall LSI is negative.

Scale formation can be minimized by reducing the concentration of calcium and magnesium (softening) or acidification which reduces the pH in sensitive areas. Another common approach is the addition of antiscalants which form complexes with the calcium and magnesium ions or delay the precipitation. All those solutions add undesirable chemicals to the water and require equipment to introduce the chemicals. An alternative approach to prevent scale is polarity reversal. In this process the functions of product and

waste stream alternate. The same compartment carries the product for some time and the waste stream later, allowing any precipitate that may have formed in one-half cycle to dissolve in the other. This process was developed for electrodialysis systems by Giuffrida [12] and described by Katz [13] as electrodialysis reversal (EDR).

In this paper we describe the implementation of the polarity reversal principle to a CDI module [14]. We focus on the characterization of the system in terms of pH and conductivity distribution within the module, the scale potential in different areas within the module and on the product quality achieved during the polarity reversal cycle. The effect of applied voltage and reversal frequency were also investigated.

EXPERIMENTAL

Cell design

The experiments were performed with a specially designed CDI unit, schematically shown in Fig. 1. It contained four anion/cation exchange membrane pairs (10 cm × 30 cm) in a serial arrangement and two electrode compartments. Accordingly, three streams of water existed during the operation: diluate (product), concentrate and electrode (waste). The spaces between each membrane pair (3 mm in thickness) in the diluate and concentrate cells were filled with a mixture of anion and cation exchange resin

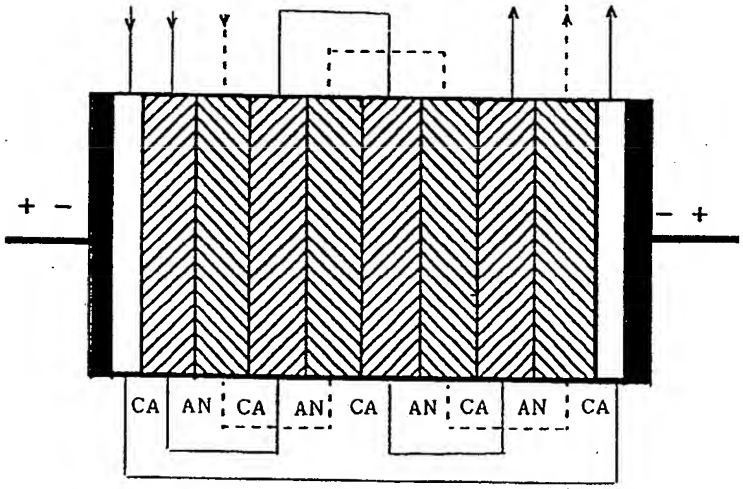

Fig. 1. A schematic representation of the CDI unit. The three different flows are represented by arrows. AN and CA are for the anion and cation exchange membranes, respectively. The solid area represents an electrode; the shaded area represents an ion exchanger.

beads. This is in contrast to a standard (non-reversal) CDI unit in which only the diluate compartments are packed with resin.

The spaces between each electrode and the adjacent membrane were not filled with ion-exchanger. Instead, a screen was used to ensure even flow distribution. The diluate and concentrate streams flowed through the appropriate compartments in a serial manner. This flow pattern created an easy way to achieve multistaging in a rather compact unit. The flow direction in these compartments was not changed upon voltage reversals. The flow through the electrode compartments was always directed from the anode to the cathode. As will be shown later, in this way the pH in the cathode compartment became more acidic and the risk of scale accumulation decreased.

In the following, the terms "anodic half cycle" and "cathodic half cycle" were assigned to the half cycles where the water inlet was adjacent to the anode or the cathode, respectively. Some of the compartments were equipped with a thin Teflon tubing located at the center. This allowed sampling of the solution for pH and conductivity monitoring of the water along the module. To ensure that sampling did not affect the processes under study, the sampling flow rate was limited to 1/50 of the total flow.

Ion exchange resins

A regenerated nuclear grade cation/anion exchange resin mixture was used. The amount of the anion to cation exchange ratio was adjusted to be equivalent. This was done by exhausting the resin mixture with 1 M NaCl solution and monitoring the pH of the solution. The pH was neutralized, if needed, by adding cation or anion exchange resin. When neutralized, the mixture contained approximately 3:2 wet volume ratio of anion to cation exchange resin.

Feed solutions

In the experiments with scale-forming components, the feed solution composition and concentration was controlled by two multichannel Minipulse 3 peristaltic pumps. They continuously introduced a solution containing a mixture of 100 g/l $CaCl_2$ and 45 g/l $MgCl_2$ and another solution of 75 g/l $NaHCO_3$. The first solution was acidified with HCl to a level which provided a feed pH of 6.8–7. When necessary, the conductivity of the feed was adjusted by pumping a solution of 300 g/l NaCl. In another series of

experiments, feed water containing only NaCl was used. In this case the conductivity was adjusted to 600 μs/cm.

The feed conductivity was monitored with an on-line Foxboro 910M Conductivity Monitor connected to a chart recorder. Total alkalinity, total hardness, magnesium and calcium concentrations were determined according to the procedures listed in the *Handbook for Water Analysis* (1979 edition, published by Hach Chemical Company). In all the experiments the Ca:Mg weight ratio was 2.5–3.

Pretreated tap water was used in all the experiments. The treatment included: 3 μ and 0.3 μ filtration, ultrafiltration, softening and scavenging of organic material. Water conductivity was usually 60 μs/cm after this treatment.

Controls

The entire operation of the system was controlled by an Allen Bradley SLC 100 Programmer Controller. The time between the reversals was controlled with an Allen Bradley 1745 Timer-Counter Access Terminal. Constant voltages were applied across the module by means of a Lambda LQD-422 dual regulated power supply.

PERFORMANCE IN THE ABSENCE OF SCALE-FORMING FACTORS

In the initial phase of this work, feed water containing NaCl only was used. This allowed the study of the processes in each compartment across the module without the risk of scaling. The behavior in each compartment was monitored at both the cathodic and the anodic half cycles.

The movement of ions in the various compartments at the two half cycles of voltage reversal is illustrated in Fig. 2. In the cathodic half cycle, the migration of Na^+ ions towards the cathode and that of the Cl^- towards the anode produced a dilute stream. The diluate compartments were indicated by the odd numbers. Similarly, the concentrate compartments were marked with the even numbers. The function of these streams was reversed upon polarity reversal during the anodic half cycle.

Fig. 2 also describes the H^+ and OH^- ions generated by water splitting occurring at the membrane/solution and the ion exchanger/solution interfaces, as well as by water electrolysis at the electrode/solution interface. This special pattern affected the pH and the conductivity of each compartment. Details are given below.

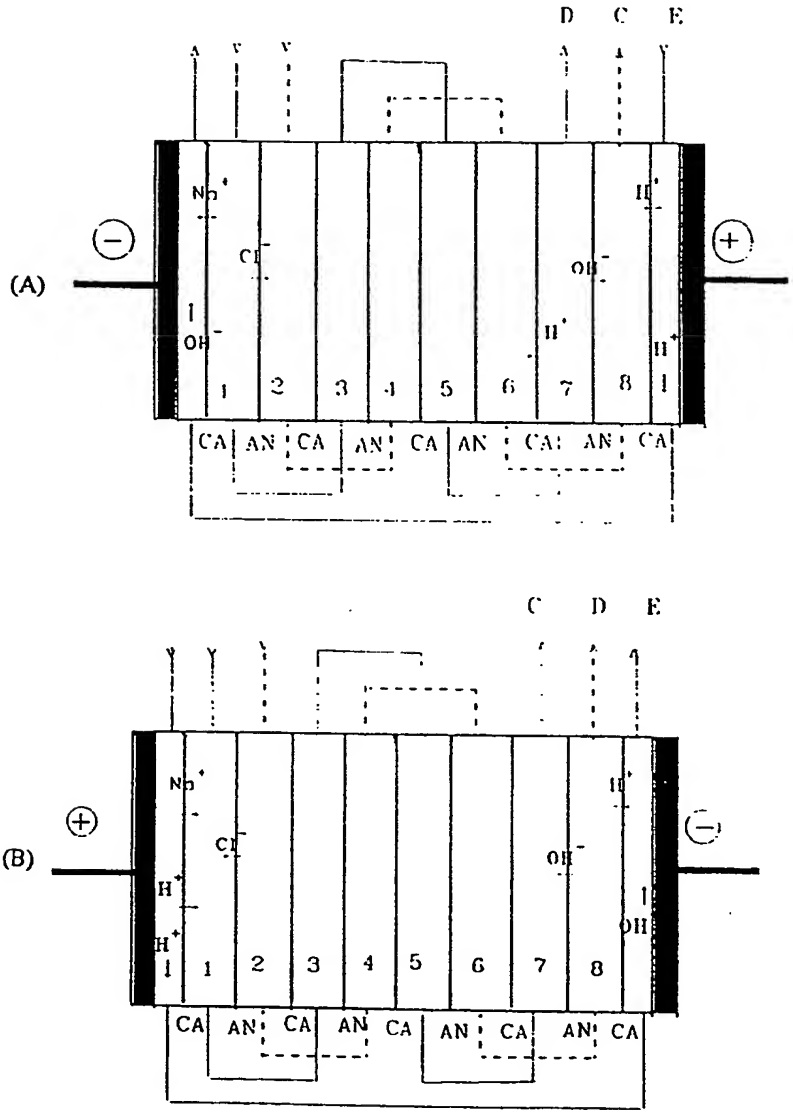

Fig. 2. Flow directions and movement of ions and water splitting ionic products in (A) the cathodic half cycle and (B) the anodic half cycle. C, concentrate; D, diluate, E, electrode streams.

Conductivity

The conductivity in compartments 1, 2, 3, 6, 7 and 8 for the two half cycles and for different voltages is shown in Fig. 3. The duration of each

half cycle was 120 min, long enough to ensure the establishment of steady-state conditions.

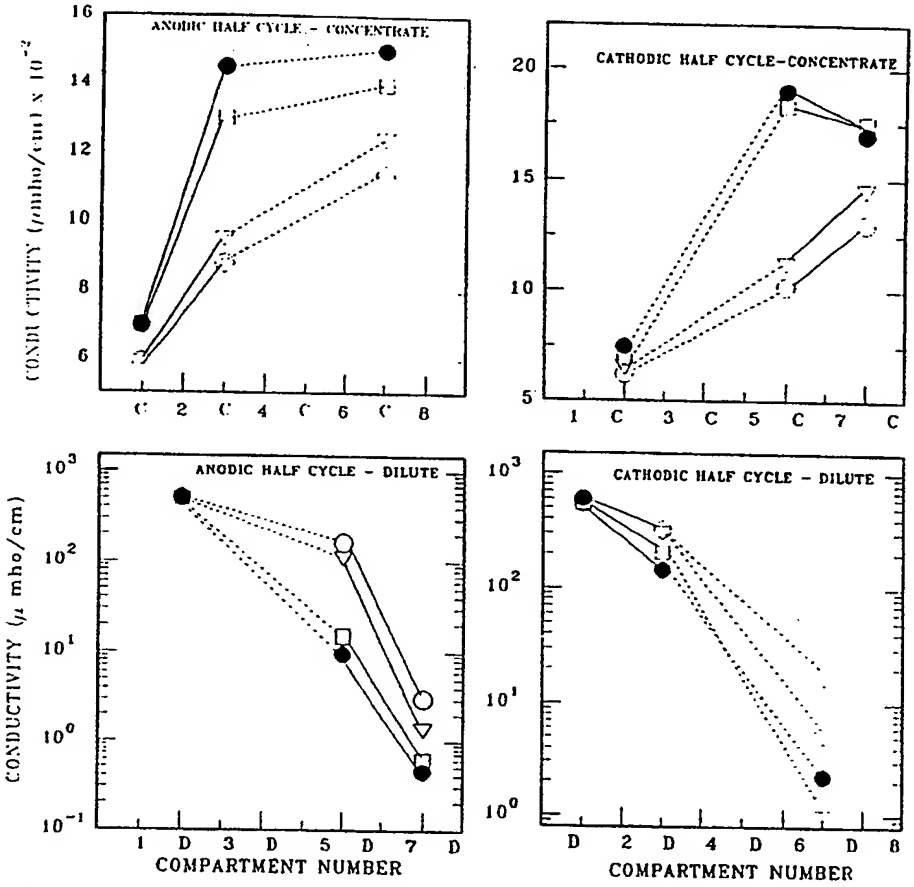

Fig. 3. Conductivity distribution along the concentrate (C) and diluate (D) streams in the cathodic and the anodic half cycles. Feed solution: 300 ppm NaCl; time between reversals, 120 min; voltage: ○ 10V, ▽ 12V, □ 18V, ● 20V.

The conductivity distribution followed the expected pattern and exhibited the alternating functions of the different compartments at each half cycle. Also the effect of the applied voltage on the product quality was apparent: the conductivity of the diluate stream decreased upon increasing the voltage. Some differences between the diluate quality attained at the two half cycles were attributed to small differences in the performance of the membranes and the ion exchangers' packing quality along the diluate and concentrate flow paths.

A typical product (diluate) water resistivity as a function of the applied voltage is given in Fig. 4. Obviously, water quality improved with the

increase in the applied voltage. It should be noted that the acceptable voltage per cell in a reversal CDI system is much higher than that commonly used in other (conventional CDI or ED) systems. This helps to compensate for the loss in product quality upon reversal.

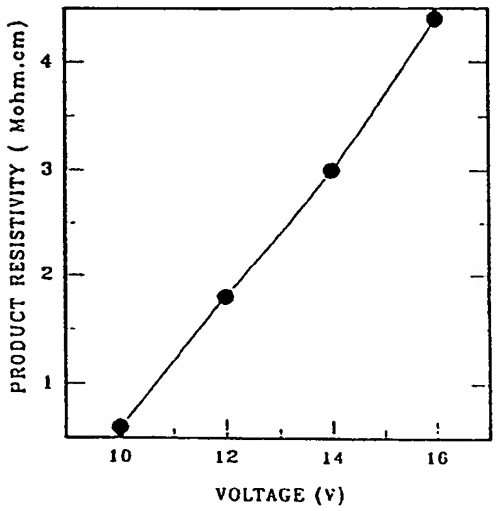

Fig. 4. Product resistivity as a function of voltage under normal operation. Feed solution was 300 ppm NaCl.

pH patterns

The pH distribution patterns are shown in Fig. 5 for the anodic and cathodic half cycles. These patterns were measured under the same conditions as those in Fig. 3 and were analyzed based on a water splitting tendency at each one of the compartments and the influence of water electrolysis at the electrode compartments and on the ions' movement regime within the module.

In the anodic half cycle, H^+ ions produced at the anode as a result of water electrolysis were transported through the first cation exchange membrane to the first concentrate compartment (number 1). The solution there became more acidic as the voltage increased.

The pH measured at the center of compartment number 3 reflect those attained at the end of the preceding concentrate compartment. A pH gradient was developed along compartment number 1 due to the accumulation of H^+ ions, resulting in considerably low pH values at the center of compartment number 3. The pH values attained within compartment number 7, which was

the last concentrate compartment, was greatly affected by water splitting in the last diluate compartment (number 8). As shown in Fig. 2, OH^- ions generated at the last diluate compartment migrated to the last concentrate compartment, resulting in a gradual increase of the pH with voltage. The concentrate effluent reached values as high as 10.5.

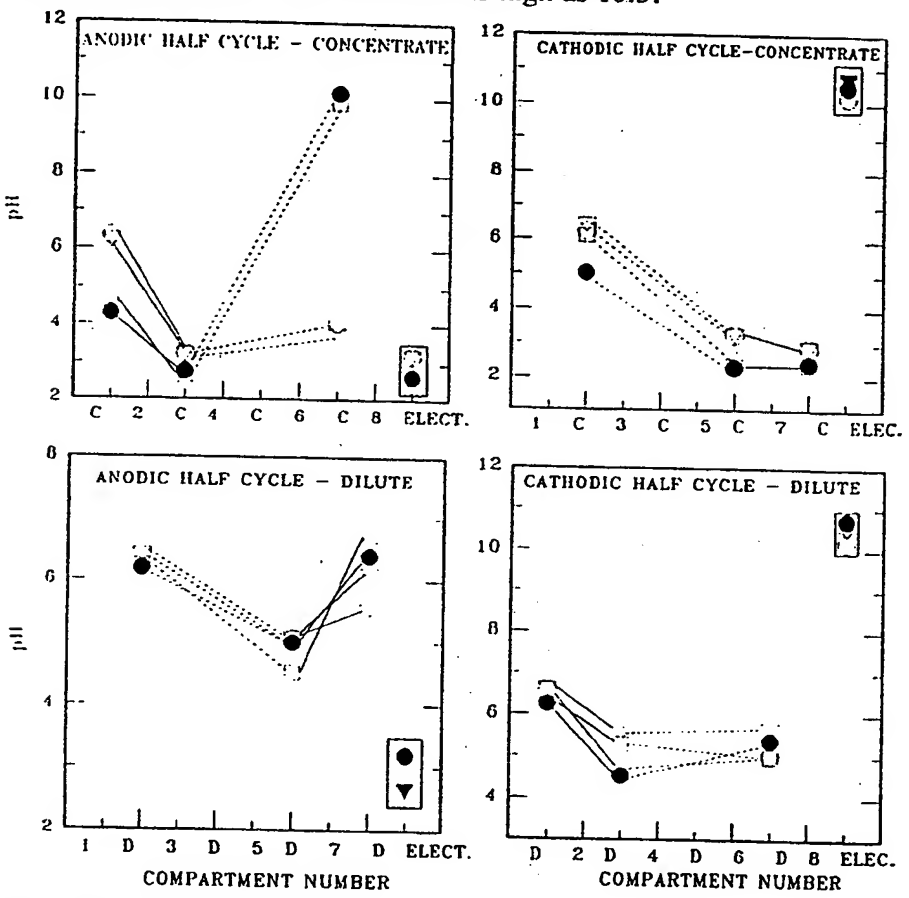

Fig. 5. pH distribution along the concentrate and diluate streams in the cathodic and the anodic half cycles. Conditions are the same as in Fig. 3. Boxed-in area is for the pH at the electrode outlet.

The pH of the diluate stream did not change significantly along the module and was in the 4.5–6.5 range. The pH values measured at the electrode effluent were acidic at the applied voltage range. Again, in accordance with Fig. 2, this was due to the large H^+ ions supply to the electrode stream by water electrolysis at the anode compartment and from compartment number 8 as a result of water splitting.

During the cathodic half cycle, no dramatic pH changes occurred at the first three compartments. However, due to water splitting in the last diluate compartment (number 7), water flowing through the third concentrate compartment (number 6) became acidic and stayed in this range. Also, the last concentrate compartment was acidic due to the larger H^+ flux coming from the adjacent anode as compared to the OH^- flux through the last anion exchange membrane. Due to the deficiency in H^+ ions in the anode compartment resulting from their migration into the last concentrate compartment, the electrode effluent was highly basic in this half cycle.

These pH patterns determine which regions within a module were expected to be the most sensitive to scale. From this point of view, it is clear that the last concentrate compartment in the anodic half cycle and the cathode compartment in the cathodic half cycle were expected to have the largest tendency to scale.

The effect of time between reversals

The effect of the time between reversals on the resistivity of the diluate effluent at the end of each half cycle is shown in Fig. 6 along with the value obtained at the same voltage under normal operation. It is apparent that the resistivities (0.54–1.1 megohm/cm) obtained under the reversal regime were lower compared with that obtained under normal operation (4.5 megohm/cm).

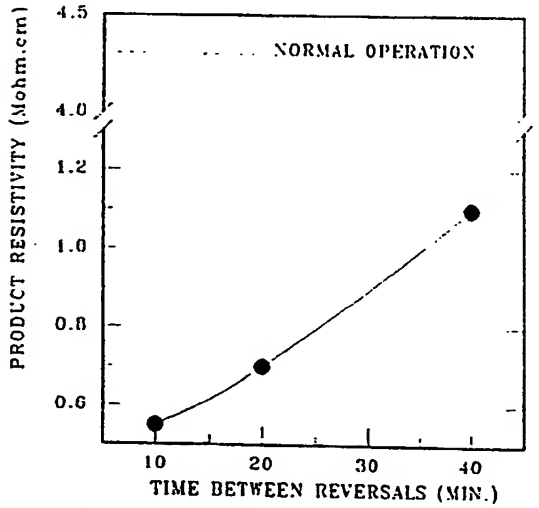

Fig. 6. Product resistivity as a function of the time between reversals. Voltage 16V; feed 300 ppm NaCl. The resistivity at normal operation is also presented.

Average water quality was also affected by the reversal of polarity in another way. Once a concentrate compartment was converted into a diluate one, it took approximately 1 min [14] until the previous (concentrated) solution was flushed out and for the resistivity to start increasing. Unless provisions are made for the disposal of the fraction of the water flowing during this time, it will be fed to the diluate stream and will lower the average water quality. It should be noted, however, that there is a lag time between the polarity reversal and the time in which valves have to be switched (when the quality of both streams is equal). If such a lag time is taken into account, the total time in which water has to be diverted to drain can be reduced substantially.

The effect of time between reversals on the pH distribution in the module is shown in Fig. 7 for the anodic and cathodic half cycles. A steady-state pattern was obtained after the module was run for a prolonged time (typically overnight) at each voltage. The development of the pH profiles with the increasing time between reversals was noticeable in particular in the anodic half cycle where at the two last concentrate compartments (numbers 5 and 7), it changed from mild acidic at the shorter times to highly basic at steady state.

These variations could be explained on the basis of the ion movement regime shown in Fig. 2. However, the following additional effects have to be taken into account: the ion exchanger beads had a damping effect on the pH of the water as it flowed through the compartments while they alternated between the concentrate and the diluate functions. As long as the time between reversals was short enough, water splitting products were adsorbed by the ion exchanger beads, and the development of extreme pH values in the module was avoided. Allowing a long time between each reversal resulted in a complete exhaustion of the beads and loss of the ability to further absorb H^+ and OH^-. This resulted in the development of extreme pH values particularly in the fifth and seventh compartments as mentioned above. The pH of the electrode stream was also affected by the time between reversals as can be observed at the anodic half cycle (Fig. 7); namely, it became more acidic as the time increased. As the degree of conversion of the ion exchangers increased (at longer times between reversals), more H^+ ions were transferred to the cathode compartment, thereby decreasing the pH of the electrode effluent. The electrode stream was not affected by changes in time between reversals during the cathodic half cycle as the electrode stream flowing through the cathode did not face any compartment within which water splitting occurred.

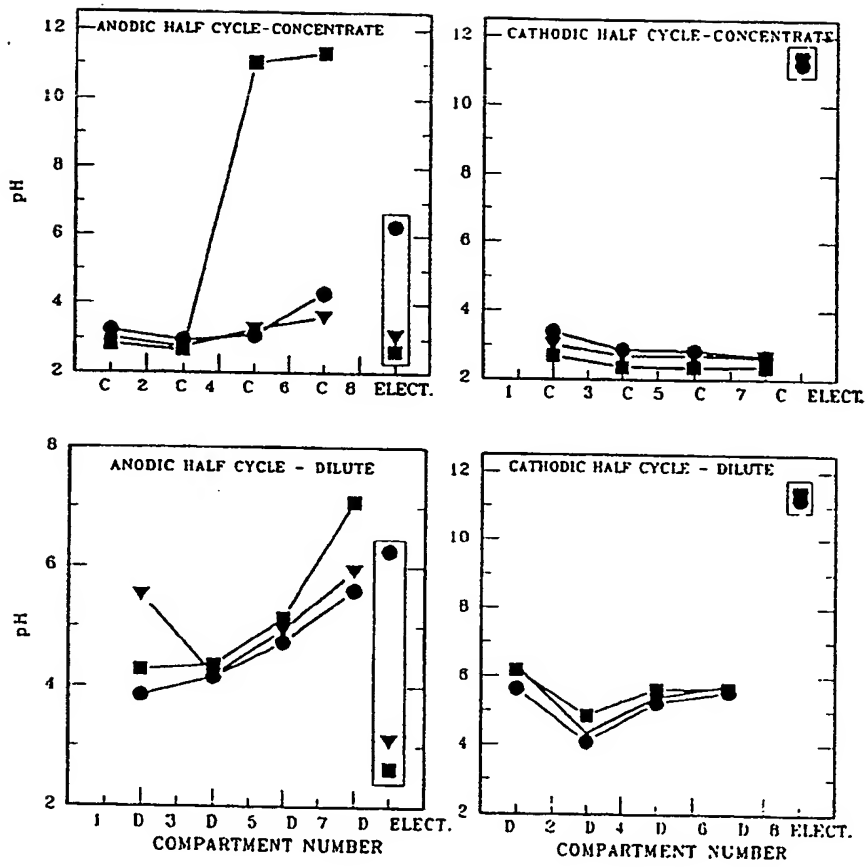

Fig. 7. pH distribution along the concentrate and diluate streams in the cathodic and the anodic half cycles at different times between reversals: ● 40 min., ▼ 67 min., ■ 720 min. Voltage 24V; feed 300 ppm NaCl. Boxed-in area is for the electrode outlet.

PERFORMANCE IN THE PRESENCE OF SCALE-FORMING COMPONENTS

A feed solution containing calcium, magnesium and alkalinity was used in this phase of the work. Typical results of the ionic concentration in the different streams are given in Table I. LSI values indicating the scale potential in each stream were also calculated. In the table, ALK, CA, MG, An and Cat are the alkalinity, calcium and magnesium concentrations, anodic and cathodic half cycles, respectively.

Table I shows the relative sensitivity for scale that the concentrate stream at the anodic half cycle as compared to that stream at the cathodic half cycle.

The obvious overall decrease in the sensitivity to scale as the concentration of the scale-forming factors in the feed decreases is also shown.

TABLE I

Typical pH, concentrations and LSI values. Operating conditions: 24V, 20 min between reversals, 200 ml/min in each stream. Concentrations are in ppm

	Feed	Concentrate		Electrodes		Diluate
		An	Cat	An	Cat	
Run 1: lower feed concentration						
ALK	18	58	5			
CA	31	78	57			
MG	17	40	34			
pH	6.7	7.9	5.2	5.9	10.4	
LSI	−1.99	+0.08	−3.86			
Run 2: higher feed concentration						
ALK	50	118	100			8
CA	96	258	209			13.4
MG	50	166	111			6
pH	7.1	8.98	7.2	6.0	9.1	5.9
LSI	−0.64	+2.00	+0.06			−3.12

Distribution of pH along the stack

The pH distribution along the module at two voltages is given in Fig. 8 for both anodic and cathodic half cycles. The pH distribution followed the same pattern as shown in Fig. 4. Since in this case the scale formation was expected, the time between reversals was not extended beyond 40 min.

A comparison between the pH distribution patterns shown in Fig. 8 and those presented in Fig. 7 for the same feed conductivity, 40 min between reversals and 24V indicates that at the anodic half cycle, higher pH values were generated in the last two concentrate compartments (number 5 and 7) in the presence of scale-forming components as compared to the case where they are absent. This phenomenon was intriguing in view of the fact that when calcium and magnesium were present, the electrical resistance of the entire module was twice as large as that in the presence of NaCl only. As a result, the current in the former case was half the value of the current

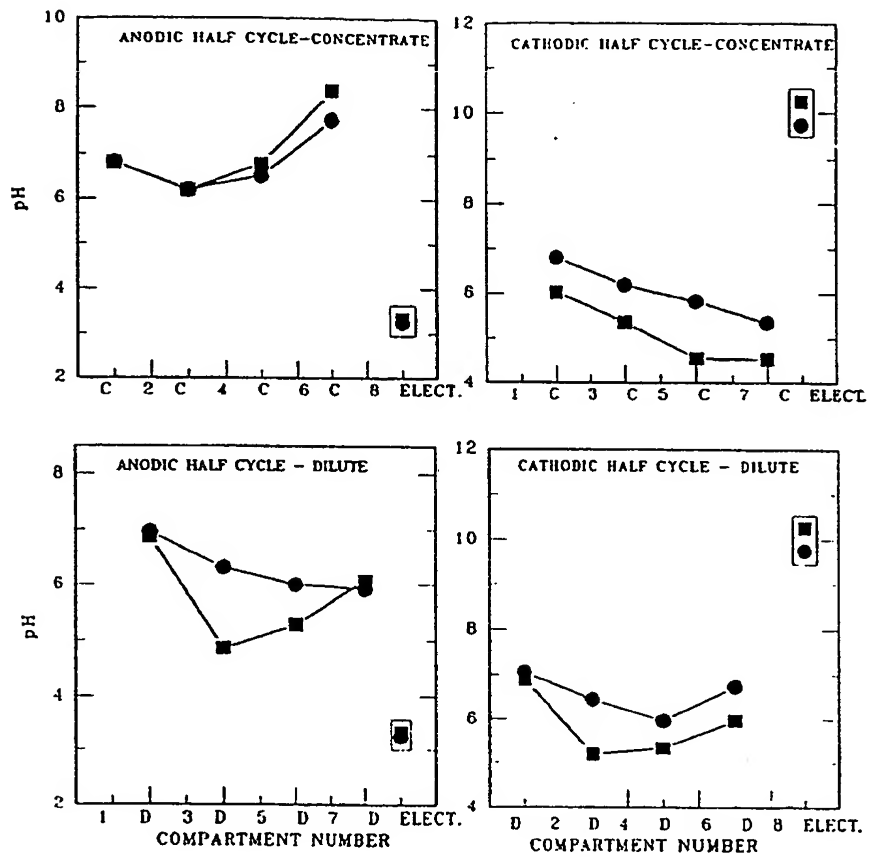

Fig. 8. pH distribution along the concentrate and diluate streams in the cathodic and the anodic half cycles at different voltages: ● 24V, ■ 32V. Time between reversals, 40 min.; feed: total hardness, 150 ppm; total alkalinity, 50 ppm; conductivity, 600 μmho/cm.

obtained in the latter, and the extent of water splitting was expected to be much smaller.

The fact that HCO_3^- ions were concentrated in the concentrate stream could not account for the higher pH values in the last concentrate compartments at the anodic half cycle because this should have resulted in a pH increase in *all* the compartments along the concentrate path.

A possible explanation may be based on the works of Oda and Yawataya and Simons [15,16] in which it was shown that calcium and magnesium ions could catalyze water splitting at the solution/membrane interface according to the following mechanism [16]:

$$Mg^{2+} + 4H_2O \Longleftrightarrow Mg(OH)_2 + 2H_3O^+$$

$$Mg(OH)_2 \Longleftrightarrow Mg^{2+} + 2OH^-$$

This mechanism is supported by the fact that the electrode stream in the anodic half cycle was more acidic in the presence of Ca^{++} ions (pH = 3.3, see Fig. 8). As compared with the case of Na^+ ions only (pH of 6.5, Fig. 7), this mechanism is supported since it shows that the transfer rate of H^+ ions generated by water splitting in compartment number 8 through the last cation exchange membrane was enhanced.

The conclusion from the last comparison is that the presence of calcium and magnesium ions in the feed water may result in an increased sensitivity to scale formation in the concentrate stream along with reduced sensitivity in the electrode stream.

The effect of the enhanced water splitting can be translated to LSI values for the concentrate and electrode streams. Two sets of pH values along with the corresponding LSI values are compared in Table II: the actual ones and those that would be generated in the absence of enhanced water splitting (namely when pH values equal to those generated in the presence of NaCl only). It should be noted that while in the "regular" case both LSI are negative, in the real case with enhanced water splitting, the LSI of the concentrate has become slightly positive.

TABLE II

LSI numbers and pH values for the anodic half cycle with pH values generated at the absence and the presence of enhanced water splitting. Other conditions are as in Fig. 8.

Water splitting conditions	Concentrate		Electrode	
	pH	LSI	pH	LSI
Regular	3.79	− 3.20	6.26	−3.24
Enhanced	7.07	+0.08	3.25	−6.10

DETERMINATION OF THE OPERATIONAL ENVELOPE

In any effort to produce the highest water quality with the smallest unit possible, it is desirable to increase voltage and time between reversal as much as possible, as long as polarity reversal can be effectively used to dissolve scale that may have formed in the concentrate or the electrode compartments. Obviously, for any given water composition there is a balance between these factors.

In an attempt to explore this balance, a series of tests was run on the same module varying the voltage per cell, the time between reversal, and the

concentration of the feed. Product water quality and formation of scale, if any, were noted. Results are summarized in Table III.

From this table it appears that for feed containing up to 150 ppm hardness, safe operation can be accomplished if voltage is kept below 8V/cell and time between reversal is no more than 40 min. This table does not give any indications as to trade-off between these parameters for other experimental conditions.

TABLE III

Performance under various voltages, time between reversal and total alkalinity

Total alkalinity	Total hardness	Time between reversal, min	Voltage/ cell volts	Prod. resist. mohm/cm	Scale formed?
20	49	10	4	.13	no
19	49	10	5	.14	no
19	49	10	6	.15	no
18	48	20	6	.20	no
19	47	40	6	.30	no
18	47	40	8	.39	yes
53	149	10	4	.11	no
47	144	10	5	.13	no
49	148	10	6	.14	no
49	146	20	6	.15	no
49	146	40	6	.24	no
38	150	20	8	.18	no
38	147	40	8	.40	yes

This experimental information, along with the detailed analysis of the localized pH distribution within the module, should be viewed only as the first step in a more extensive study on the performance of a CDI module under polarity reversal conditions.

ACKNOWLEDGMENT

The authors wish to thank J. Denoncourt, G. Ganzi, A. Giuffrida and L. Woo for their help and advice during the performance of this research.

REFERENCES

1 W.R. Walters, D.W. Wieser and L.J. Marek, Concentration of radioactive aqueous wastes — Electromigration through ion-exchange membranes, Electrochim. Acta, 47(1) (1955) 61–67.

2 V.A. Shaposhnik, A.K. Reshetnikova, R.I. Zolotareva, I.V. Drobysheva and N.I. Isaev, Denaturalization of water by electrodialysis with ion exchange packing between the membranes, Zhurnal Prikladnoi Khimii, 46 (1955) 1–67.

3 E. Glueckauf, Electrodeionization through a packed bed, Brit. Chem. Engineering, (1959) 646–651.

4 Z. Matejka, Continuous production of high purity water by electro-deionization, J. Appl. Chem. Biotechnol., 21 (1971) 117–120.

5 O. Kedem, Reduction of polarization in electrodialysis by ion conducting spacers, Desalination, 16 (1975) 105–118.

6 E. Korngold, Electrodialysis in water desalination and the influence of ion exchange resin introduction into the apparatus, Int. Symp. Brackish Water, (1976) 209.

7 G. Ganzi, Y. Egozy, A. Giuffrida and A. Jha, High purity water by electrodeionization: The performance of the Ionpure™ continuous deionization system, Ultrapure Water J., 4(3) (1987) 43.

8 G.C. Ganzi, Electrodeionization for high purity water production, In: K.K. Sirkar and D.R. Lloyd (Eds.), AIChE Symposium Series, New Materials for Processes for Separation, New York, 84(261) (1988) 73.

9 G.C. Ganzi, Water purification and recycling using the Ionpure CDI process, AIChE Summer National Meeting, Paper 41c, 1991.

10 G.C. Ganzi, Ionpure CDI electrodeionization systems: New products and process for the development of high purity water. In: M. Abe et al. (Eds.), New Developments in Ion Exchange, Proceedings of the International Conference on Ion Exchange ICIE'91, Tokyo, 1991, pp. 317–322.

11 R.A. Pisigan, Jr., and J.E. Singley, Evaluation of water corrosively using the Langelier Index and relative corrosion rate models, Material Performance, 24(4) (1985) 26–36.

12 A.J. Giuffrida and E.J. Parsi, Method for preventing scale buildup during electrodialysis operation, U.S. Patent 3,341,441, 1967.

13 W.A. Katz, The electrodialysis reversal, Desalination, 28 (1979) 31–40.

14 A.J.Giuffrida, G.C. Ganzi and Y. Oren, Electrodeionization apparatus and module, U.S. Patent 4,946,071, 1990.

15 Y. Oda and T. Yawataya, Neutrality-disturbance phenomenon of membrane-solution systems, Desalination, 5 (1968) 129.

16 R. Simons, Electric field effects on proton transfer between ionizable groups and water in ion exchange membranes, Electrochimica Acta, 29 (1984) 151–158.